Supplemental Figure 1

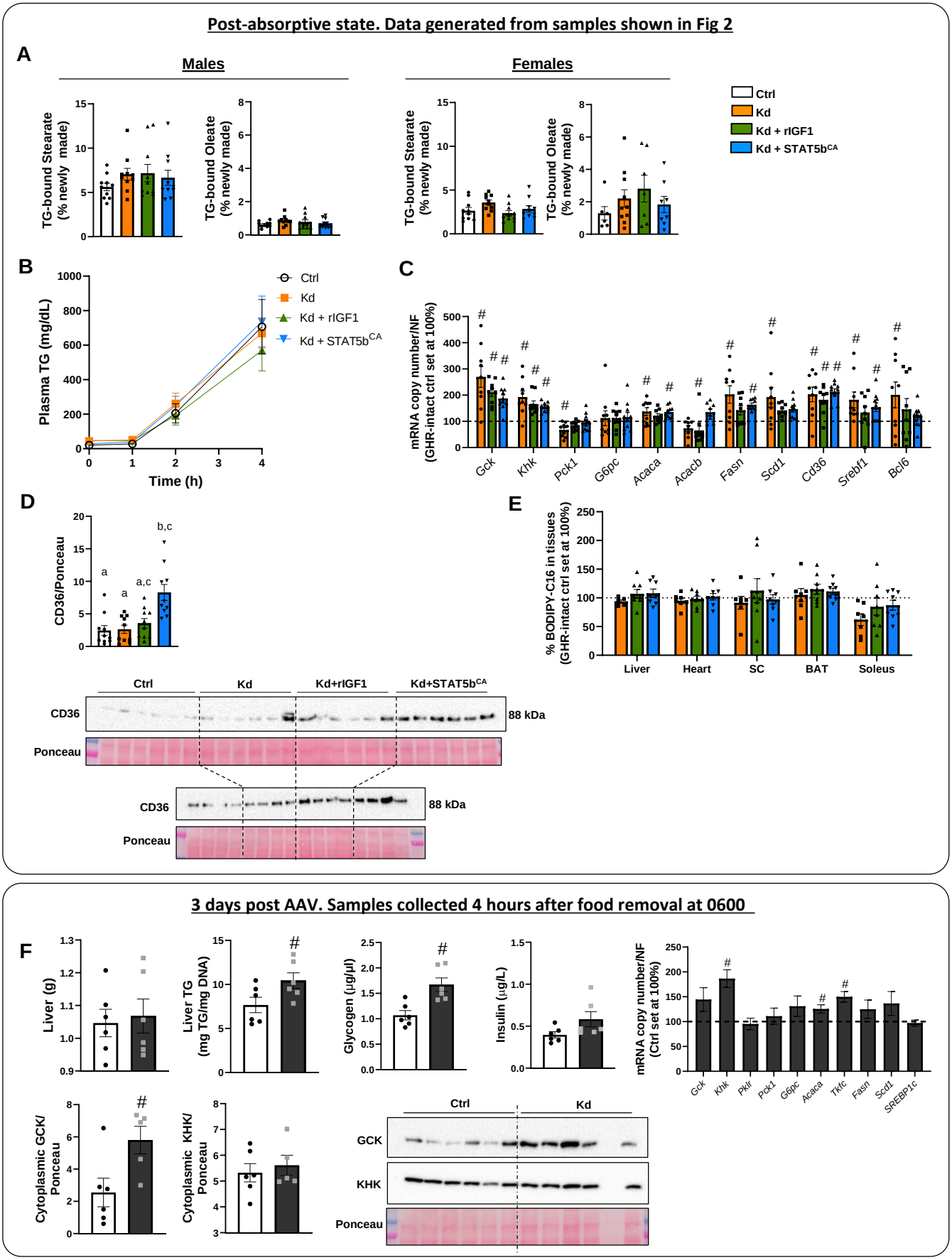

Supplemental Figure 1: (A) Percentage of newly formed hepatic stearate and oleate associated with TG in male and female aHepGHRkd mice without or with IGF1 or STAT5b^{CA} (n=10 mice/group). **(B)** Rate of hepatic VLDL-TG secretion after tyloxapol injection (500 mg/kg i.p.) in males 7d post-aHepGHRkd, without or with rIGF1 or STAT5b^{CA} maintenance, with study conducted after 4h food removal starting at 0800 h (n=6-7 mice/group). **(C)** RNA-seq validation of some glycolytic, gluconeogenic and fatty acid synthesis-related genes assessed by qPCR. GHR-intact controls were set at 100% (n=10 mice/group). **(D)** CD36 protein levels assessed by Western Blot (n=10 mice/group). **(E)** Percentage of BODIPY-C16 uptake in different tissues in males 7d post-aHepGHRkd, without or with rIGF1 or STAT5b^{CA} maintenance, where GHR-intact controls are set at 100% (n=7-8 mice/group). **(F)** Impact of 3 days aHepGHRkd on liver weight, liver TG, glycogen, insulin, cytoplasmic glucokinase (GCK) and ketohexokinase (KHK) protein levels (assessed by Western Blot), and mRNA expression levels (assessed by qPCR; n=6 mice/group). Values are represented as mean ± SEM, with all data points included. #, indicates values that differ from GHR-intact controls, $p<0.05$.

Supplemental Figure 2

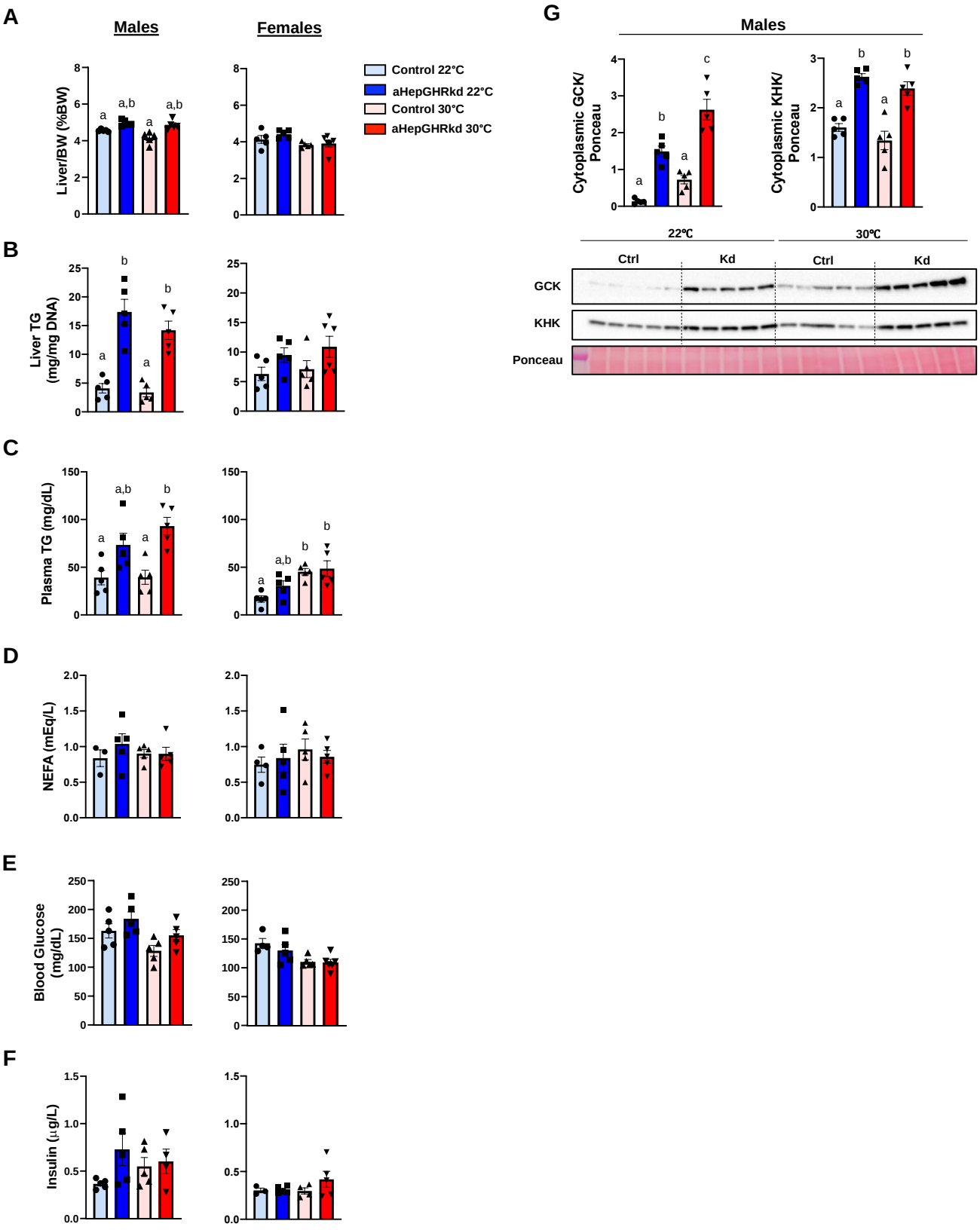

Supplemental Figure 2: Male and female GHR$^{fl/fl}$ mice (10-12 weeks of age) were acclimated to temperature controlled cabinets set at 22°C or 30°C for one week, then injected with AAV-TBGp-Cre or AAV-TBGp-Null. Seven day later tissues were collected for analysis. (A) Liver weight at sacrifice represented as percentage of the body weight. **(B)** Liver triglyceride (TG) content. **(C-F)** Circulating levels of plasma TG, non-esterified fatty acids (NEFA), glucose and insulin levels. **(G)** Cytoplasmic glucokinase (GCK) and ketohexokinase (KHK) protein levels in males, assessed by Western Blot. Protein levels are normalized by Ponceau staining. Values are represented as mean ± SEM, with all data points included (n=5-6 mice/group). Values that do not share a common letter (a, b, c) are statistically different, $p < 0.05$.

Supplemental Figure 3

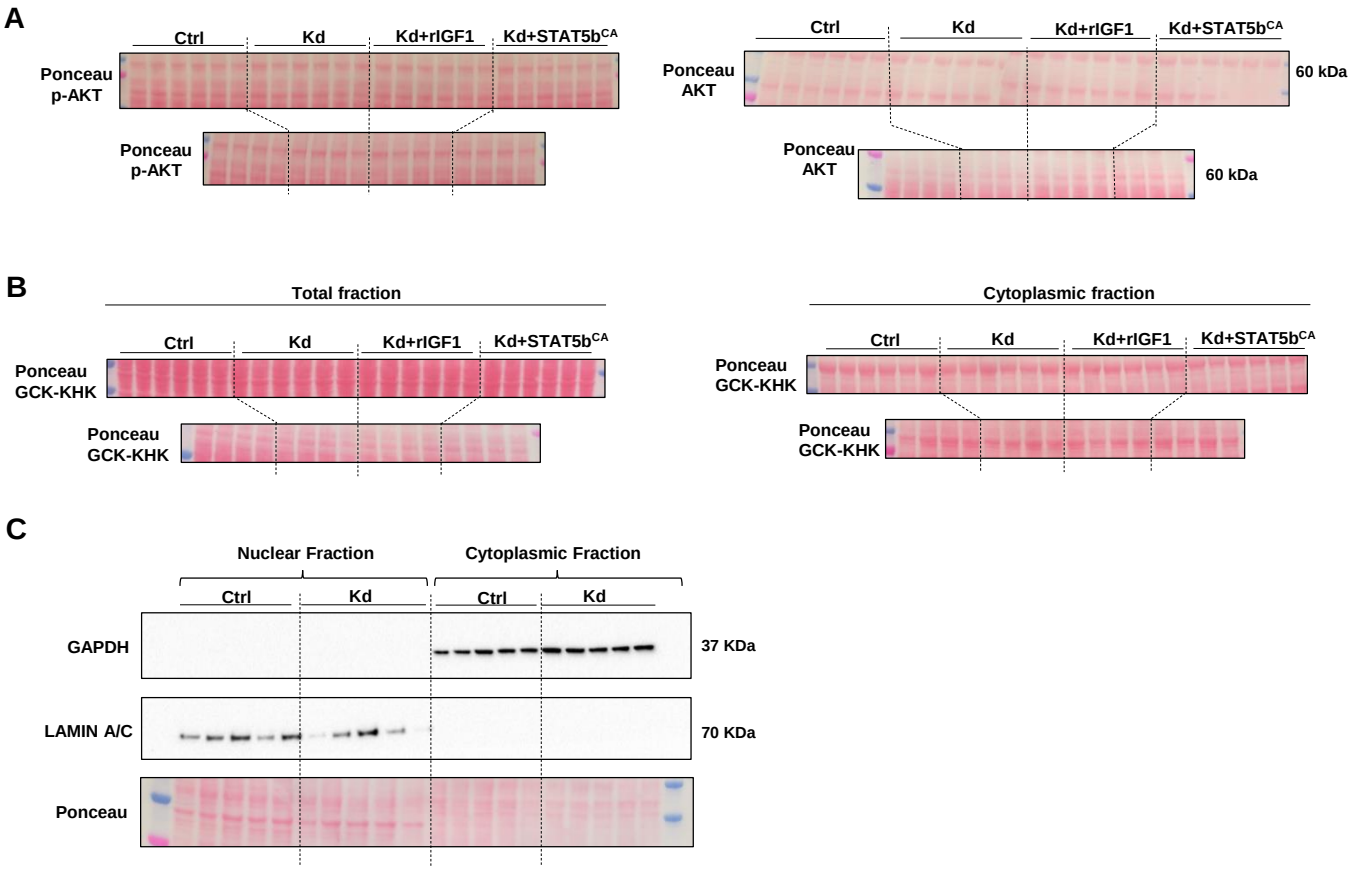

Supplemental Figure 3: (A) p-AKT and AKT ponceaus in Ctrl, Kd, Kd + rIGF1 and Kd + STAT5b^{CA} from membranes shown in Figure 2A and assessed by Western Blot. **(B)** Total and cytoplasmic glucokinase (GCK) and fructokinase (KHK) ponceaus from membranes shown in Figure 2G and assessed by Western Blot. **(C)** Validation of nuclear and cytoplasmic fractions using GAPDH as cytoplasmic marker and LAMIN A/C as nuclear marker in a subset of control (Ctrl) and aHepGHRkd (Kd) mice from the postabsorptive experiment injected with deuterated water (n=5 mice/group).

Supplemental Figure 4

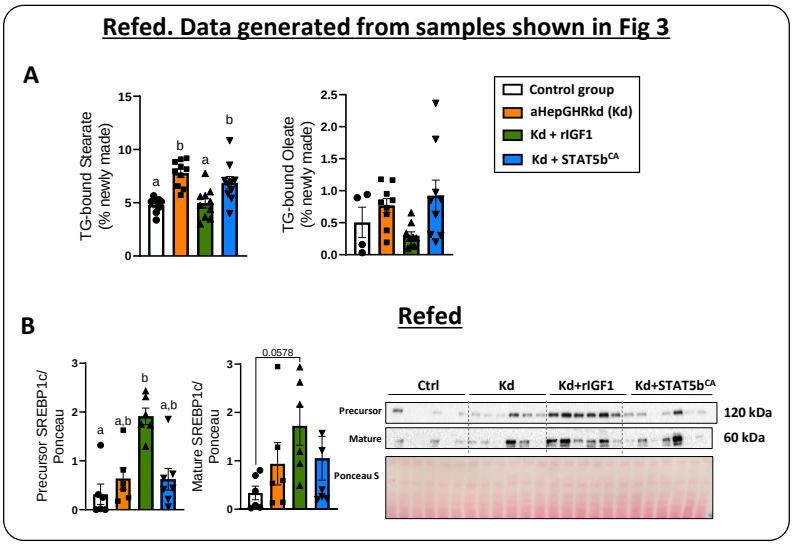

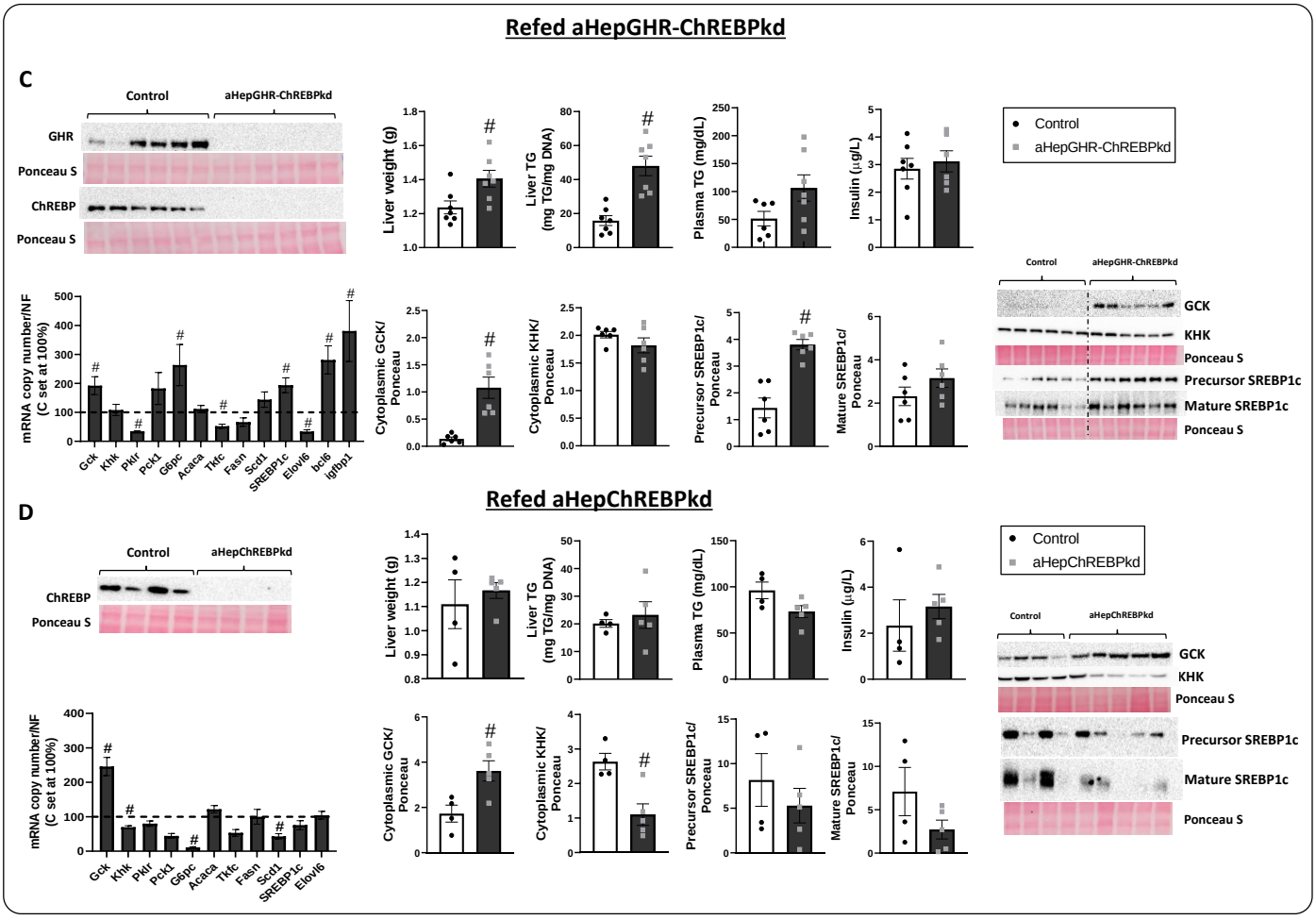

Supplemental Figure 4: (A-B) Additional data from mice that were refed after overnight fasting, as shown in Fig. 3 **(A)** Percentage of newly formed hepatic stearate and oleate (n=10 mice/group). **(B)** Precursor and mature SREBP1c protein levels assessed by Western Blot (n=10 mice/group). Values that do not share a common letter (a, b, c) are statistically different ($p < 0.05$). ChREBP$^{fl/fl}$ mice were purchased from Jackson Labs (#032381) and crossbred with GHR$^{fl/fl}$ mice, or maintained as a separate colony. **(C)** Impact of aHepGHR-ChREBPkd or **(D)** aHepChREBPkd on liver weight, liver TG, plasma TG, insulin, mRNA expression levels, cytoplasmic GCK and KHK, precursor and mature SREBP1c, 6 hours of refeeding, after an overnight fast. Values are represented as mean ± SEM, with all data points included. #, indicates values that differ from GHR or GHR-ChREBP intact controls, $p<0.05$.

Supplemental Figure 5

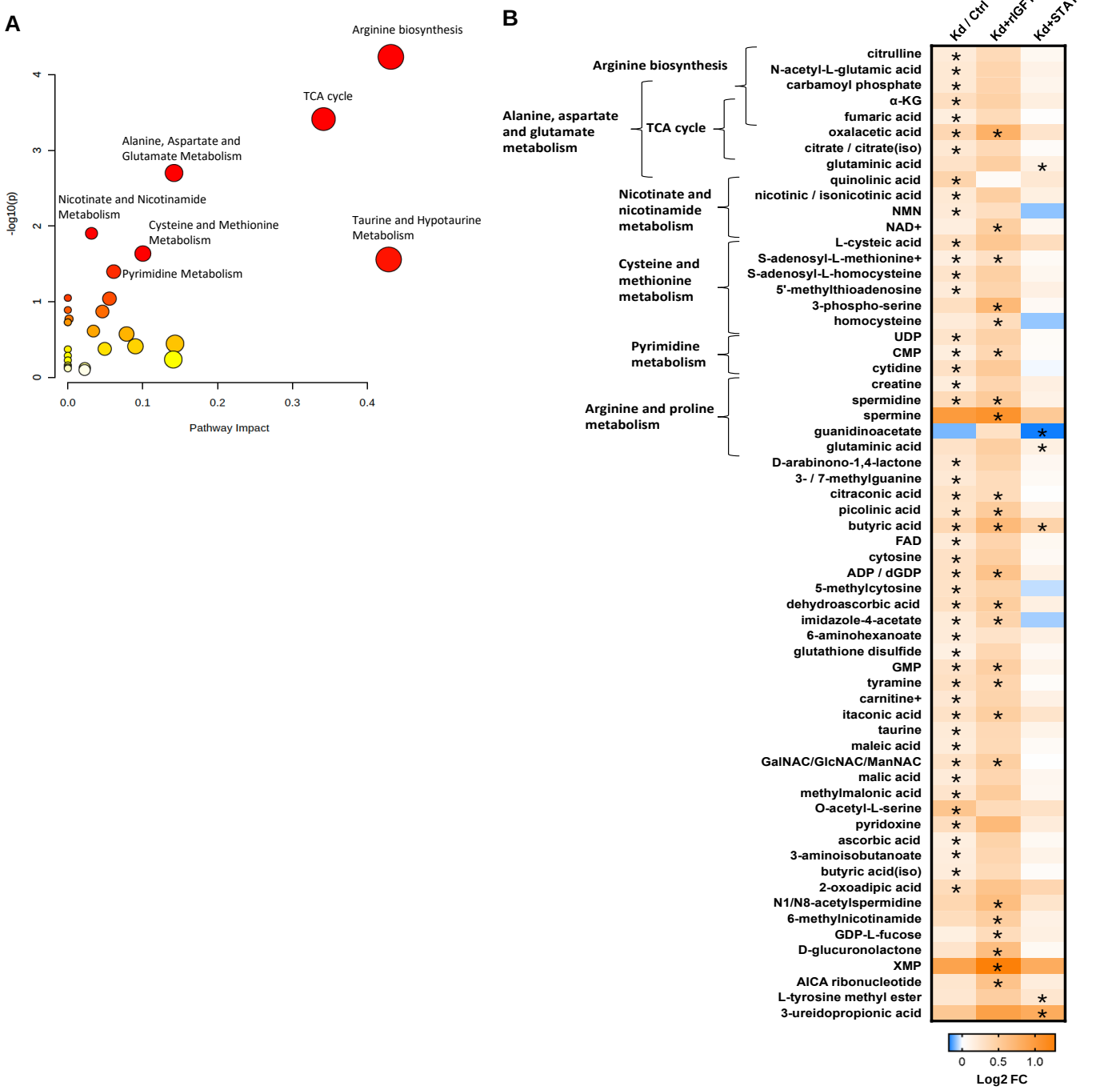

Supplemental Figure 5: Metabolomic analysis of livers from refed aHepGHRkd male mice without or with IGF1 or STAT5b^{CA} replacement. Liver samples same as in-text Fig 3**. (A)** Metabolomic pathway analysis from refed aHepGHRkd male mice without or with IGF1 or Stat5b^{CA}. Metabolic pathways are displayed as circles. The color of each circle is based on *p*-values (darker colors indicate more significant changes of metabolites in the corresponding pathway), whereas the size of the circle corresponds to the pathway impact score. The most impacted pathways having high statistical significance scores are annotated. **(B)** Heatmap of altered metabolites and the pathways they are associated with. (n=5 mice/group). *$p < 0.05$.

Supplemental Figure 6

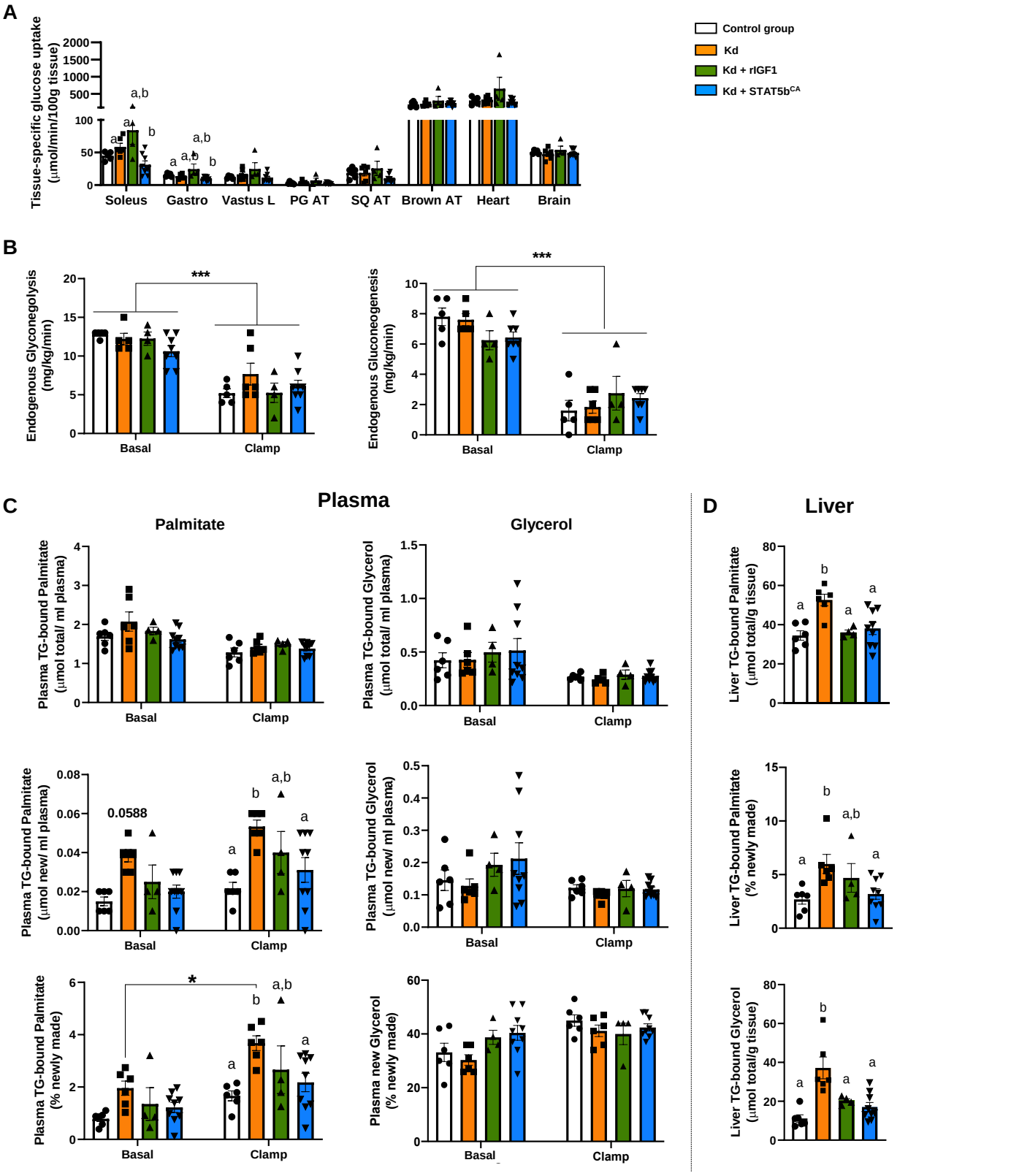

Supplemental Figure 6: Additional endpoints measured after hyperinsulinemic-euglycemic clamps in aHepGHRkd male mice with or without IGF1 or STAT5b^{CA} replacement (associated with in text Fig. 4), (A) Tissue-specific glucose uptake in muscle (soleus, gastrocnemius, vastus lateralis), adipose tissue (perigonadal, subcutaneous, brown), heart and brain. **(B)** Glycogenolysis and gluconeogenesis, before and after the clamp. **(C)** Plasma total (μmol total/ml plasma), new (μmol new/ml plasma), and % newly made TG-bound palmitate and glycerol before and after the clamp. **(D)** Liver total TG-bound palmitate and glycerol (μmol/g tissue) and percentage newly made TG-bound palmitate. Values are represented as mean ± SEM, with all data points included (n=4-9 mice/group). Values that do not share a common letter (a, b, c) are statistically different ($p < 0.05$). * $p<0.05$, *** $p<0.001$

Supplemental Figure 7

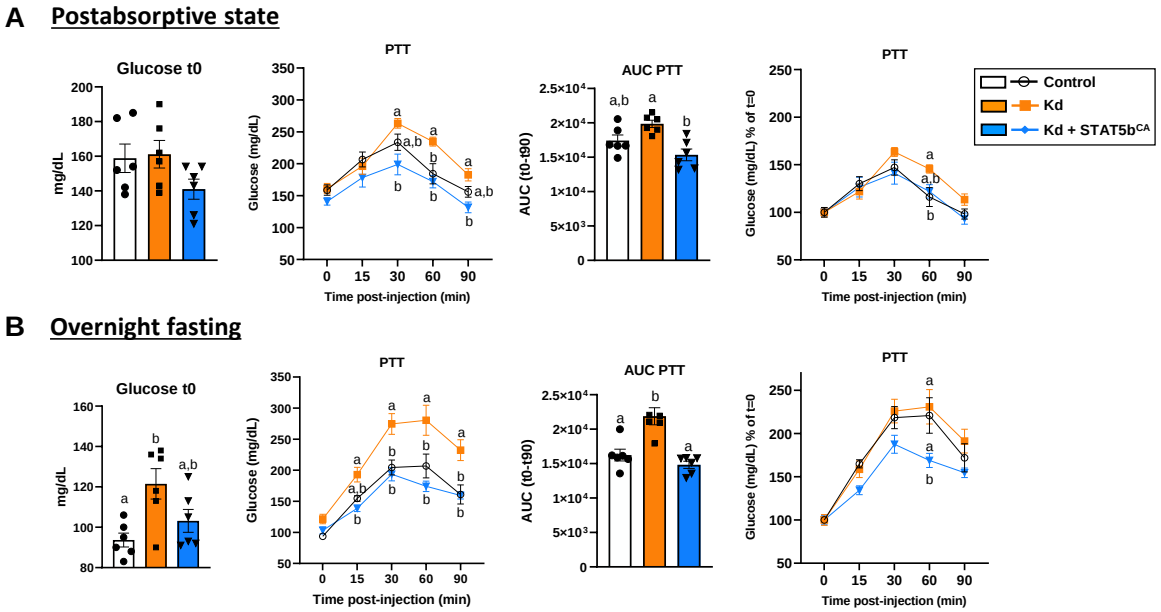

Supplemental Figure 7: Impact of aHepGHRkd without or with STAT5b^{CA} on pyruvate tolerance test (PTT) assessed in the post-absorptive state (A) and after overnight fast (B) 7 days after AAV injection (n=5/group). Glucose was measured before and 15, 30, 60 and 90 minutes after pyruvate intraperitoneal injection (2g/kg). Values are represented as mean ± SEM, with all data points included. Values that do not share a common letter (a, b, c) statistically differ ($p < 0.05$).